BIOCHEMISTRY
including biophysical chemistry & molecular biology

Article

pubs.acs.org/biochemistry

Interactions of Indocyanine Green and Lipid in Enhancing Near-Infrared Fluorescence Properties: The Basis for Near-Infrared Imaging *in Vivo*

John C. Kraft and Rodney J. Y. Ho*

Department of Pharmaceutics, University of Washington, Seattle, Washington 98195, United States

ABSTRACT: Indocyanine green (ICG) is a near-infrared (NIR) contrast agent commonly used for *in vivo* cardiovascular and eye imaging. For medical diagnosis, ICG is limited by its aqueous instability, concentration-dependent aggregation, and rapid degradation. To overcome these limitations, scientists have formulated ICG in various liposomes, which are spherical lipid membrane vesicles with an aqueous core. Some encapsulate ICG, while others mix it with liposomes. There is no clear understanding of lipid−ICG interactions. Therefore, we investigated lipid−ICG interactions by fluorescence and photon correlation spectroscopy. These data were used to design stable and maximally fluorescent liposomal ICG nanoparticles for NIR optical imaging of the lymphatic system. We found that ICG binds to and is incorporated completely and stably into the lipid membrane. At a lipid:ICG molar ratio of 250:1, the maximal fluorescence intensity was detected. ICG incorporated into liposomes enhanced the fluorescence intensity that could be detected across 1.5 cm of muscle tissue, while free ICG only allowed 0.5 cm detection. When administered subcutaneously in mice, lipid-bound ICG in liposomes exhibited a higher intensity, NIR image resolution, and enhanced lymph node and lymphatic vessel visualization. It also reduced the level of fluorescence quenching due to light exposure and degradation in storage. Lipid-bound ICG could provide additional medical diagnostic value with NIR optical imaging for early intervention in cases of lymphatic abnormalities.

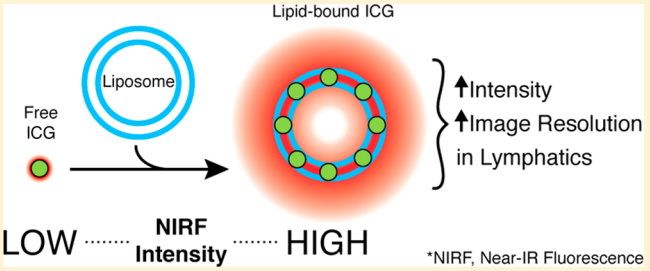

Indocyanine green (ICG) is the only near-infrared (NIR) fluorescent dye approved by the U.S. Food and Drug Administration (FDA) and European Medicines Agency (EMA) for human use.[1] With its 820 nm NIR emission wavelength, ICG is considered a good *in vivo* contrast agent with minimal interference from blood and tissue autofluorescence (~500−600 nm). It is indicated for determining cardiac output, hepatic function, and liver blood flow, and for ophthalmic angiography. ICG is used off-label or in research to visualize anatomical structures filled with fluid (for example, blood, cerebrospinal fluid, lymph, or urine) or as a contrast agent for vascular, renal, or excretory pathways.[2] In aqueous environments, ICG molecules aggregate and ICG fluorescence readily degrades.[3−6] In blood, ICG binds to plasma proteins, enhancing its fluorescence intensity. *In vivo* ICG fluorescence intensity and duration may vary with fluctuating plasma protein and lipoprotein concentrations and interindividual variation.

To overcome the protein binding dependency, scientists have attempted to add ICG to hydrophobic polymers, serum albumin, and nanoparticles, including liposomes. Recent reports on ICG and liposomes with diverse physiochemical characteristics prepared by various procedures have demonstrated the potential of ICG−lipid particles for optical imaging of lymphatic function,[7,8] sentinel lymph nodes (SLNs),[9] vascular permeability,[10] and angiogenesis.[11] However, most of these liposomes with varying compositions containing ICG were prepared without a full understanding of the interactions between ICG and lipids. Under certain conditions, ICG can physically interact with phospholipids in the liposome membrane and modify the stability and quantum yield of ICG as well as the structure and stability of the lipid membrane. ICG may also be encapsulated in the aqueous compartment of liposomes. These properties and variations could profoundly impact optical NIR imaging quality and the ability to provide medical diagnostic value.

Not all liposomes are alike; some may consist of phospholipids with different headgroups and fatty acyl chains, while others may include cholesterol or other additives, all of which can alter a liposome's physiochemical properties.[12] Because of a high degree of overlap between the absorption and emission spectra of ICG, ICG exhibits concentration-dependent fluorescence quenching (self-quenching). It is therefore important to define not only the lipid−ICG interactions but also the optimal density of ICG molecules within a lipid bilayer that exhibits both maximal fluorescence intensity per ICG molecule and minimal self-quenching. On the basis of the biochemical characteristics of ICG and lipid−ICG interactions, a stoichiometric range of the lipid:ICG molar ratio that prevents self-quenching and maximizes the fluorescence yield can be achieved through systematic studies. Binding of ICG to

Received: January 6, 2014
Revised: February 6, 2014
Published: February 10, 2014

   dx.doi.org/10.1021/bi500021j | *Biochemistry* 2014, 53, 1275−1283

the lipid has been assumed through indirect evidence to stabilize ICG fluorescence and protect the ICG molecule from oxidation, resulting in an enhanced fluorescence intensity.[4,9,13−16] However, the interactions between ICG and lipid have yet to be studied.

Therefore, the goals of this study are to elucidate the lipid−ICG interactions that influence ICG fluorescence intensity and ICG−lipid complex stability and to evaluate liposomal ICG as an *in vivo* imaging agent. We found that ICG binds to lipid and in the process stabilizes and enhances its fluorescence properties, overcoming the dependency on protein binding. Compared to free ICG, ICG embedded in a lipid membrane enhanced the visualization of the popliteal lymph node and downstream lymph nodes in mice and allowed light to be transmitted through 1.5 cm of muscle tissue. In addition, these liposomal ICG nanoparticles, produced by an efficient and scalable preparation procedure that incorporates nearly 100% of ICG, had excellent light exposure and storage stability.

EXPERIMENTAL PROCEDURES

Chemicals. Indocyanine green (ICG, $C_{43}H_{47}N_2NaO_6S_2$, sodium 2-{7-[3,3-dimethyl-1-(4-sulfonatobutyl)benz[*e*]indolin-2-ylidene]hepta-1,3,5-trien-1-yl}-3,3-dimethyl-1-(4-sulfonatobutyl)benz) was purchased from Sigma-Aldrich (St. Louis, MO). 1,2-Distearoyl-*sn*-glycero-3-phosphocholine (DSPC), 1,2-distearoyl-*sn*-glycero-3-phosphoethanolamine-*N*-methoxy-polyethylene glycol-2000 ($DSPEmPEG_{2000}$), and L-α-phosphatidylcholine (Egg PC) were purchased from Avanti Polar Lipids (Alabaster, AL). Other reagents were analytical grade or higher.

Methods. *Liposome Preparation.* Control or empty liposomes and liposomal ICG were prepared by thin film hydration and sonication. Briefly, DSPC dissolved in $CHCl_3$ and $DSPEmPEG_{2000}$ dissolved in a $CHCl_3/CH_3OH$ mixture [3:1 (v/v)] were mixed (9:1 molar ratio) in a sterile test tube. The mixture was then dried under N_2 gas and reduced pressure into a thin film, which was vacuum desiccated overnight at room temperature. The thin film was rehydrated with 0.9% NaCl, 20 mM $NaHCO_3$ buffer at pH 7 (final lipid concentration of 20 mM) at 60 °C for 3 h. The liposome diameter was reduced to approximately 50−80 nm via a 15 min bath sonication at 55 °C. For liposomal ICG, ICG dissolved in 100% CH_3OH was added to the lipid mixture prior to it being dried into a thin film. ICG self-quenching[17] was reduced, and the density of ICG in the lipid membrane was optimized. The mean diameters of liposomes and liposomal ICG were obtained by particle size analysis with photon correlation spectroscopy (PCS) on a PSS-NICOMP 380 ZLS instrument (Particle Sizing Systems, Port Richey, FL). The ζ potential was measured on the same instrument. The ICG incorporation efficiency was evaluated by separation of lipid-bound and free ICG by equilibrium dialysis. All experiments were performed under dark conditions, and light exposure was avoided.

90° Light Scattering of ICG Adsorbed to Liposomes. ICG dissolved in 100% CH_3OH was incubated with liposomes in plastic micronic tubes at lipid:ICG molar ratios of 25:1 to 500:1 for 20 min before being diluted 25-fold with 0.9% NaCl and 20 mM $NaHCO_3$ buffered at pH 7 to minimize ICG−lipid interactions. The 90° light scattering was then measured on a Hitachi (Troy, MI) F-4500 fluorescence spectrophotometer. The set parameters were as follows: λ_{ex} and λ_{em} values of 660 nm and excitation and emission slit widths of 2.5 and 5 nm, respectively. Samples were stored away from light at room temperature during observation.

Fluorescence. Fluorescence measurements were performed on a Victor[3] V 1420-040 Multilabel Plate Reader (Perkin-Elmer, Waltham, MA) with a tungsten−halogen continuous wave lamp (75 W, spectral range of 320−800 nm) and excitation (769 ± 41 nm) and emission (832 ± 37 nm) filters (Semrock, Rochester, NY) using 100 μL of sample in flat bottom, untreated 96-well plates (Grenier Bio-one, Monroe, NC).

Light Exposure and Storage Stability. For light exposure stability, samples of free ICG and liposomal ICG at 2.0 μM ICG were exposed to overhead fluorescent tube lighting for 12 h. Fluorescence measurements were recorded at 0, 6, and 12 h. For storage stability, samples were placed in the dark at 4 °C for up to 313 days. Fluorescence measurements were recorded at five different time points for free ICG and at 10 different time points for liposomal ICG. The time-dependent decay of ICG fluorescence was analyzed on the basis of an exponential decay model with GraphPad Prism version 6.0 (GraphPad Software, San Diego, CA). The data were expressed as $t_{1/2}$ (half-life) and k (rate constant).

Tissue Depth Penetration. Cuboid chicken breast tissue phantoms of three different depths (0.5, 1.0, and 1.5 cm) were used to assess ICG fluorescence detection through tissue. Tissue cuboids were placed over capillary tubes [70 μL capacity, 75 mm length, 1.2 mm inner diameter (Fisher Scientific, Hampton, NH)] filled with 50 μL of 30 μM free ICG or liposomal ICG. White light and NIR images were captured within 15 min of the preparation of capillary tubes and tissue cuboids using a custom NIR charge-coupled device (CCD) camera built by Hamamatsu Photonics K.K. (Hamamatsu, Japan). Fluorescence intensity mean values of select areas, on a scale of 0 to 255 with 255 being the maximal brightness, were obtained with the analysis function in Adobe Photoshop CS4 (Adobe Systems Inc., San Jose, CA).

In Vivo NIR Lymphatic Imaging in Mice. Mice were kept under pathogen-free conditions, exposed to a 12 h light−dark cycle, and received food *ad libitum* prior to imaging. All procedures were approved by the University of Washington Institutional Animal Care and Use Committee.

Three mice were anesthetized with 1.5% isoflurane, shaved to remove fur, and placed in a supine position on a 37 °C heat pad underneath a custom NIR CCD camera. Precontrast images were taken to confirm the absence of autofluorescence. Forty microliters of lipid-bound ICG in liposomes (250:1 lipid:ICG molar ratio) or free ICG was injected subcutaneously into the top of both rear feet (12.5 μM ICG in 0.9% buffered saline in each foot, totaling 1.0 nmol of ICG/mouse). Immediately following injections, both feet were placed under gentle even pressure. Images were acquired for up to 120 min prior to euthanasia by cervical dislocation under anesthesia, upon which the skin was surgically opened.

RESULTS

Liposomal Lipid−ICG Interactions. To evaluate the interactions between ICG and lipid, we incubated empty (no ICG) liposomes with varying concentrations of ICG. If ICG molecules in solution bind to lipids in the membrane, it will cause liposomes to cross-link and aggregate, resulting in an increase in the apparent size of the membrane that can be detected by a change in 90° light scattering and an increase in particle size. In a preliminary experiment, we first tested

liposomes composed of egg-derived phosphatidylcholine (Egg PC) (containing mixed-length fatty acyl chains) and observed an increase in light scattering intensity as the ICG concentration was increased, indicating that ICG induced liposome aggregation. We next used liposomes with a well-defined phospholipid composition, DSPC containing two symmetrical C18 fatty acyl chains and $DSPEmPEG_{2000}$ (9:1 molar ratio), to perform systematic studies. A fixed lipid concentration in liposomes of 10 μM was allowed to interact with varying ICG concentrations for 20 min at 25 °C; the reaction was stopped by 25-fold dilution with a buffered solution. The mixture was subjected to 90° light scattering analysis and photon correlation spectroscopy (PCS) to estimate particle size.

The 90° light scattering intensity is expected to be low when particles are in the single, nonaggregated form and to increase with aggregation. However, when lipid aggregates become too large, they may fall off the light path or electrons in a particle may not oscillate together in phase and cause intraparticle destructive interference, resulting in an apparent decline in scattering intensity. As shown in Figure 1A, empty liposomes (lipid only) have a low scattering intensity, and free ICG (ICG only) has a consistent scattering intensity near zero regardless of the ICG concentration. When liposomes and ICG (L-ICG) were mixed together, at low ICG concentrations (20−30 nM) a minimal light scattering intensity similar to that of the empty liposome control (lipid only) was detected. The scattering intensity of L-ICG increases approximately 1.5-fold when the ICG concentration increases from 30 to 70 nM (Figure 1A). There is a minor decline in scattering intensity at 40 nM ICG; however, it is still significantly higher than at 20−30 nM ICG. At high concentrations (100−400 nM ICG), the scattering intensity declines as aggregates become larger. Figure 1B depicts a schematic drawing of the proposed aggregate formation that leads to an initial increase in light scattering intensity followed by a decrease in intensity as the particle becomes exceedingly large. These data were confirmed by aggregate size analysis with PCS. As shown in Figure 1C, at an initial ICG concentration of 20 nM, the particle diameter is similar to that of empty liposomes (~100 nm). The apparent liposomal ICG size increases greater than 3-fold at ICG concentrations of 20−100 nM. The apparent size fluctuates around a 300 nm diameter at ICG concentrations between 30 and 100 nM and then increases to ~400 nm at 400 nM ICG. In the region of 30−400 nM ICG, we detected a small population of smaller but distinct liposomal−ICG particles with consistent diameters of 60−90 nm (data not shown).

Collectively, these data indicate that ICG binds to lipid presented in empty preformed liposomes and leads to liposome aggregates, detected as an apparent increase in particle size, and a discontinuous increase in light scattering intensity. On the basis of the lipid concentration of 10 μM and ICG concentrations of 20−50 nM, these data give rise to a lipid:ICG molar ratio estimated to be between 200:1 and 500:1 that produces maximal lipid aggregation and an apparent increase in particle size.

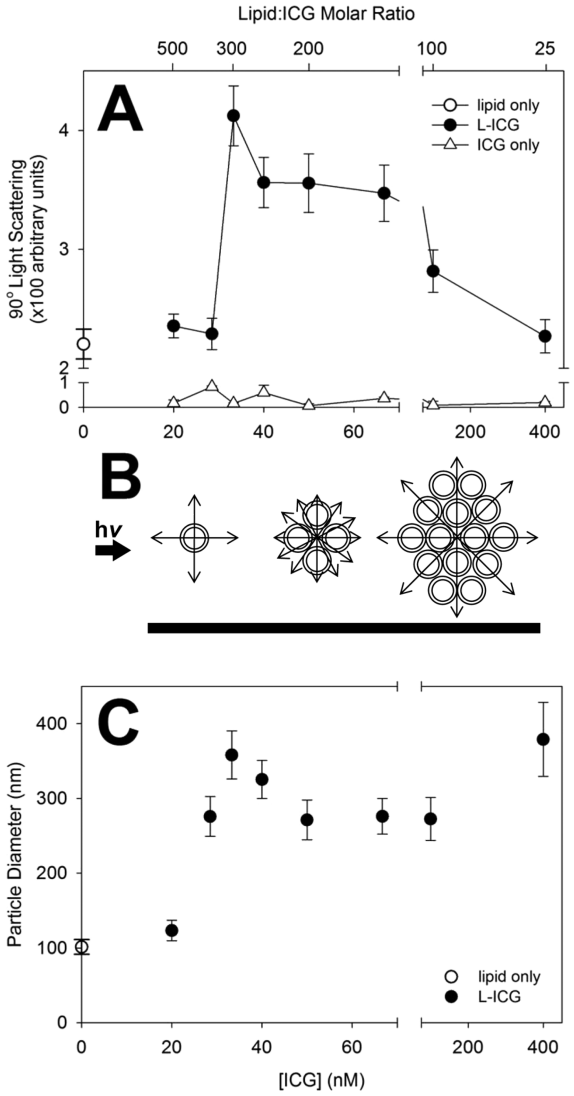

Figure 1. ICG concentration-dependent liposome aggregation and apparent size increase. (A) Effect of ICG concentration on the 90° light scattering intensity of liposomes. A fixed concentration of liposomes was incubated with varying ICG concentrations in a fixed volume. At 20 min, mixtures were diluted to stop the reaction and the 90° light scattering intensity was measured with a fluorometer as described in Experimental Procedures: (○) empty lipid only liposomes, (●) lipid-bound ICG (L-ICG), and (△) free ICG only. Each data point is the mean ± SD of 10 replicates. (B) Schematic drawing of light scattering efficiency detected by the photomultiplier tube (PMT; bold horizontal bar) 90° to the incident light ($h\nu$) path as liposomes aggregate and increase the diameter of the particle. (C) Effect of ICG concentration on particle size analysis by photon correlation spectroscopy of liposomes. Following collection of the data depicted in panel A, particle size analysis was performed as described in Experimental Procedures: (○) empty lipid only liposomes and (●) lipid-bound ICG (L-ICG). Each data point is the mean ± SD from digital autocorrelation calculations following data collection for 8 min.

Impact of Liposomal Lipid−ICG Interactions on ICG Fluorescence. We next determined the impact on the fluorescence intensity caused by binding of ICG to lipid. We used the lipid:ICG molar ratio range from 125:1 to 25000:1. Because of the self-quenching of ICG, the reaction mixture was diluted 20-fold with a buffered solution to the linear ICG concentration range of 0.01−2.0 μM. As shown in Figure 2, the presence of lipid in the mixture increases the fluorescence intensity of ICG at equivalent ICG concentrations. As the ICG concentration increases from 0.01 to 1.0 μM, the fluorescence intensity progressively widens for the mixture containing lipid versus the control. At 0.1, 0.5, and 1.0 μM ICG, the fluorescence intensity increased by 10.0-fold (65720 vs 6600), 4.3-fold (261640 vs 61360), and 2.8-fold (346610 vs 122530),

dx.doi.org/10.1021/bi500021j | Biochemistry 2014, 53, 1275−1283

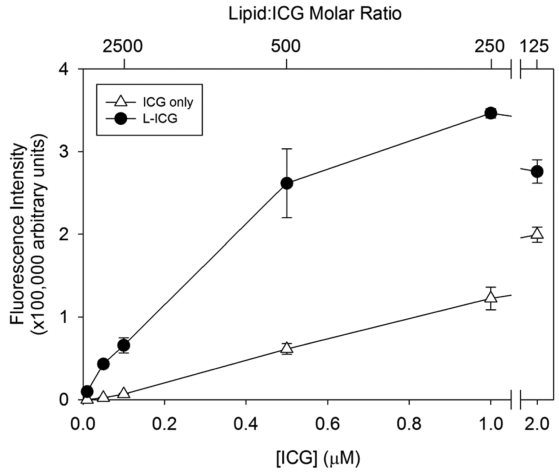

Figure 2. Increased fluorescence intensity of lipid-associated ICG. A fixed concentration of liposomes was incubated with varying ICG concentrations in a fixed volume. At 20 min, mixtures were diluted 20-fold with a buffered solution to stop the reaction, and the fluorescence intensity was measured with a fluorometer as described in Experimental Procedures: (△) free ICG only and (●) lipid-bound ICG (L-ICG). Each data point is the mean ± SD of eight replicates.

respectively. At 2.0 μM ICG, the lipid-mediated enhancement of the ICG fluorescence intensity was smaller, and an only 1.4-fold increase (275820 vs 199420) was observed. At a fixed lipid concentration of 250 μM and 0.5, 1.0, and 2.0 μM ICG, the equivalent lipid:ICG molar ratios for these values are 500:1, 250:1, and 125:1, respectively (Figure 2). Therefore, the optimal lipid:ICG molar ratio that exhibits the highest fluorescence intensity is estimated to range from 125:1 to 500:1. This estimate is consistent with data collected from 90° light scattering and PCS size analysis. These values, derived from ICG and preformed liposome interactions, were used as the target range for subsequent ICG liposome preparation and characterization studies.

Incorporation of ICG into Lipid Membranes To Stabilize and Maximize ICG Fluorescence. Instead of adding ICG in solution to lipid as admixtures in a buffered solution, we mixed ICG and lipid together in an organic solution, first, then removed the solvent, and rehydrated the sample in buffer to form liposomes in which ICG had been inserted or embedded. ICG has a significant overlap in absorption and emission spectra (Figure 3A) and consequently exhibits self-quenching potential at high concentrations. Thus, we made liposomes embedded or incorporated with different concentrations (densities) of ICG incorporated into the lipid membrane. If the ICG density is too high, the proximity between ICG molecules may induce self-quenching because of concentration-dependent molecular interactions.[17] Moreover, ICG incorporated into lipid without exposure to water would provide a higher fluorescence than ICG molecules exposed to water, which quenches ICG fluorescence. Eight lipid:ICG molar ratios ranging from 100:1 to 500:1 were evaluated. Figure 3B represents the fluorescence intensity per unit of ICG slope at typical ICG concentrations for three lipid-bound ICG samples (equivalent to molar ratios of 100:1, 250:1, and 350:1) and a soluble ICG control. At 0.01−2.0 μM ICG, the fluorescence intensity appears to increase linearly. Note that the slope of the 250:1 line is the steepest, followed by the slopes of the 350:1, 100:1, and ICG only samples. To determine the optimal lipid:ICG molar ratio, we evaluated the slope of the line for each formulation (for the sake of clarity, only three of eight total lines are presented in Figure 3B).

The slope equals the fluorescence intensity per micromolar ICG. As shown in Figure 3C, because of a decrease in ICG density and self-quenching, the fluorescence intensity per ICG (slope) increases as the lipid:ICG molar ratio increases from 100:1 to 250:1, at which point the maximum is reached. The fluorescence intensity per ICG then decreases at 300:1 and 350:1, followed by a significant decrease at 500:1. Thus, we observed the peak fluorescence intensity per ICG at a lipid:ICG molar ratio of 250:1.

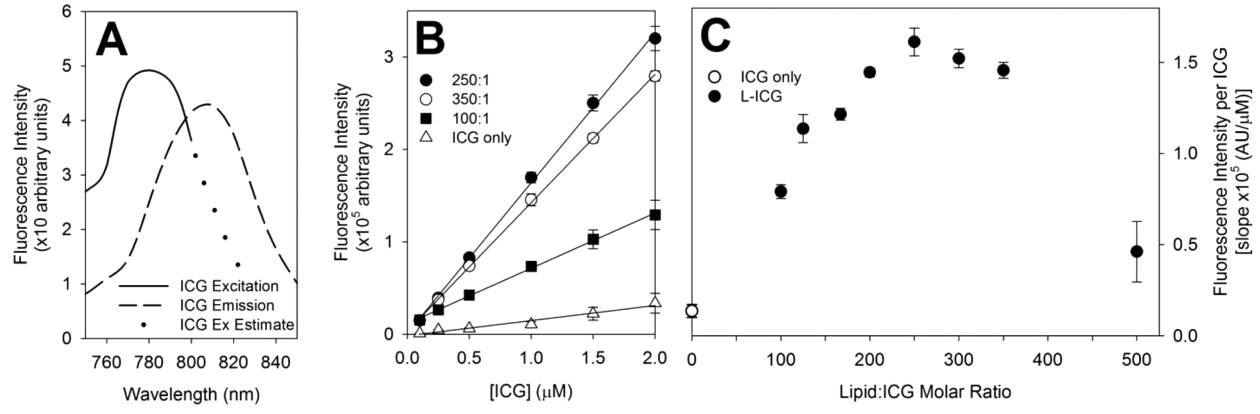

Figure 3. Optimization of the lipid:ICG molar ratio to maximize ICG fluorescence yield. (A) Excitation (—) and emission (– – –) spectra of ICG in aqueous buffer. The dotted line extending the excitation spectra is an estimate based on ref 3. (B) Effects of the lipid:ICG molar ratio on the ICG fluorescence yield (fluorescence intensity per micromolar ICG). Lipid-bound ICG with varying lipid:ICG molar ratios was prepared, and their fluorescence intensity per unit ICG was measured at the indicated concentrations. Only three of eight liposomal ICG formulations are presented for the sake of clarity; their data points are labeled according to their lipid:ICG molar ratios: (●) 250:1, (○) 350:1, and (■) 100:1 lipid:ICG molar ratios and (△) ICG only. Each fluorescence intensity data point is the mean ± SD of eight replicates. (C) Effects of lipid:ICG molar ratio on fluorescence yield. The data from panel B were used to calculate the slope (fluorescence intensity per micromolar ICG) and plotted vs the lipid:ICG molar ratio: (○) free ICG only and (●) lipid-bound ICG (L-ICG) in liposomes at varying molar ratios. Each data point is the mean ± SD of six replicates.

dx.doi.org/10.1021/bi500021j | *Biochemistry* 2014, 53, 1275−1283

As the 250:1 lipid:ICG molar ratio exhibits the highest fluorescence intensity per ICG, we characterized the 250:1 formulation using particle size analysis by photon correlation spectroscopy (PCS) and particle surface charge (ζ potential) analysis by electrophoretic light scattering (ELS). The 250:1 formulation consisted of a monodisperse population of particles with a 56.8 ± 4.4 nm diameter and a −33.1 ± 3.1 mV ζ potential. Equilibrium dialysis indicated the ICG incorporation efficiency was 97.8 ± 0.6%. Because of reproducible and almost complete incorporation of ICG, this formulation was selected without further purification for subsequent *in vitro* and *in vivo* studies.

Effects of Lipid Incorporation on Enhancing ICG Stability for Light Exposure and Storage. We next evaluated the stability of liposomal ICG in 4 °C storage and under light exposure to simulate the environment in clinical settings. As shown in Figure 4, the fluorescence intensity of liposomal ICG decreases to 87.6 ± 0.5% of the initial value after a 6 h light exposure and experiences no further decrease after 12 h ($t_{1/2}$ = 67.5 ± 11.8 h; k = 0.011 ± 0.002 h^{-1}). In contrast, the fluorescence intensity of free ICG in solution decreases to 2.5 ± 0.5% of its initial value after a 6 h light exposure ($t_{1/2}$ = 0.036 ± 0.005 h; k = 19.2 ± 2.7 h^{-1}), indicating the light instability of ICG in aqueous solutions.

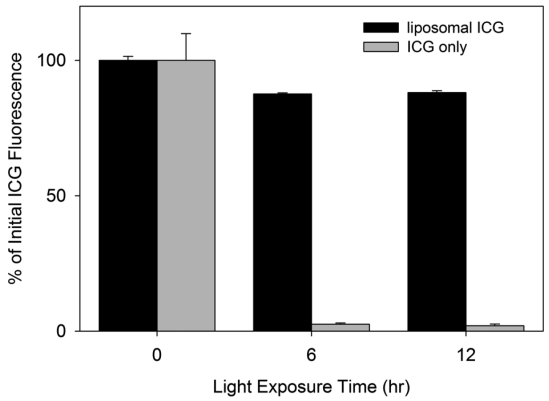

Figure 4. Lipid-bound ICG in liposomes reduces ICG fluorescence quenching due to light exposure. Liposomal ICG and free ICG were exposed to overhead fluorescent light for 12 h. ICG fluorescence was recorded at 6 and 12 h as described in Experimental Procedures. Black bars represent data for liposomal ICG and gray bars data for ICG only. Each data point is the mean ± SD of eight replicates.

To evaluate longer-term storage stability, we kept liposomal ICG in the dark at 4 °C and measured the fluorescence intensity multiple times over 313 days. As shown in Figure 5 and Table 1, ~78.2 ± 2.8% of the initial fluorescence intensity was recorded after liposomal ICG had been stored for 8 months [$t_{1/2}$ = 394 days (95% CI, 360−434 days); k = 1.76 × 10^{-3} day^{-1} (95% CI, 1.60 × 10^{-3} to 1.93 × 10^{-3} day^{-1})]. However, for free ICG in buffer, only 0.3 ± 0.2% of the initial ICG fluorescence was observed after storage for 8 months [$t_{1/2}$ = 1.19 days (95% CI, 1.14−1.25 days); k = 582 × 10^{-3} day^{-1} (95% CI, 554 × 10^{-3} to 609 × 10^{-3} day^{-1})].

Enhanced NIR Imaging of Liposomal ICG *in Vitro*. To compare the fluorescence signal intensity between liposomal ICG (250:1 lipid:ICG molar ratio formulation) and free ICG, we prepared chicken breast cuboids with increasing muscle tissue thicknesses of 0.5, 1.0, and 1.5 cm (Figure 6F). We filled all capillary tubes (75 mm in length, 1.2 mm in inner diameter)

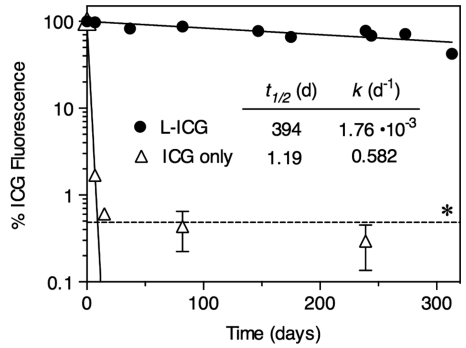

Figure 5. Stability of lipid-bound ICG in storage. Lipid-bound ICG in liposomes and free ICG were stored in the dark at 4 °C for up to 313 days, and ICG fluorescence was analyzed at indicated time points: (△) free ICG and and (●) lipid-bound ICG (L-ICG). The time course data were analyzed on the basis of an exponential decay model, and the half-life, $t_{1/2}$ (days), and rate constant, k (inverse days), values are listed. The dashed line indicates the limit of detection. Each data point is the mean ± SD of three to eight replicates.

Table 1. Storage Stability Kinetics[a]

	% ICG fluorescence[b] (8 months)	$t_{1/2}$ (days)	k (×10^{-3} day^{-1})
liposomal ICG[c]	78.2 ± 2.8	394 (360, 434)	1.76 (1.60, 1.93)
free ICG[d]	0.3 ± 0.2	1.19 (1.14, 1.25)	582 (554, 609)

[a]Stored in the dark at 4 °C. [b]Mean ± SD of samples (N = 2 each) stored for 8 months. [c]$t_{1/2}$ (95% CI) and k (95% CI) calculated from multiple time points (N = 10) over 313 days. [d]$t_{1/2}$ (95% CI) and k (95% CI) calculated from multiple time points (N = 5) over 239 days.

with 50 μL of 30 μM ICG (1.5 nmol of ICG) (Figure 6B). As shown in Figure 6A, the intensity of the capillary tube filled with liposomal ICG is 3.2-fold higher than that of free ICG (intensity means of 111.7 and 34.5, respectively). When the sample was placed under three tissue cuboids, with an increasing depth from left to right, free ICG fluorescence (top three cuboids) was detectable only across a 0.5 cm depth (top left cuboid; intensity mean of 9.0), not through greater depths; liposomal ICG fluorescence (bottom three cuboids) was detectable across 0.5, 1.0, and 1.5 cm depths (intensity means of 112.1, 77.3, and 10.0, respectively) (Figure 6C). Further analysis indicates that only liposomal ICG in capillary tubes can be detected across 1.5 cm of muscle tissue (intensity means for 0.5, 1.0, and 1.5 cm depths of 100.9, 68.0, and 15.2, respectively) (Figure 6E,F).

Effects of Liposome-Bound ICG on NIR Lymphatic Image Resolution in Mice. With the stable and optimized liposomal ICG formulation, we performed *in vivo* proof-of-principle optical imaging experiments in mice. To compare free and liposomal ICG, we subcutaneously administered ICG in 40 μL (0.5 nmol of ICG), in either free or lipid-bound form, to the mouse's left or right foot (Figure 7A). After 6 min, only the foot that received liposomal ICG (but not free ICG) exhibited a detectable popliteal node through the skin (Figure 7A). Only when the image was recorded below the skin were both popliteal lymph nodes detectable. The ICG intensity mean of the popliteal lymph node that received free ICG was 37.0 compared to a value of 208.1 for that treated with liposomal ICG (data not shown). To further compare the lymphatic image resolution of free ICG and liposomal ICG, in another set of mice, we administered ICG to both feet either in free or

dx.doi.org/10.1021/bi500021j | *Biochemistry* 2014, 53, 1275−1283

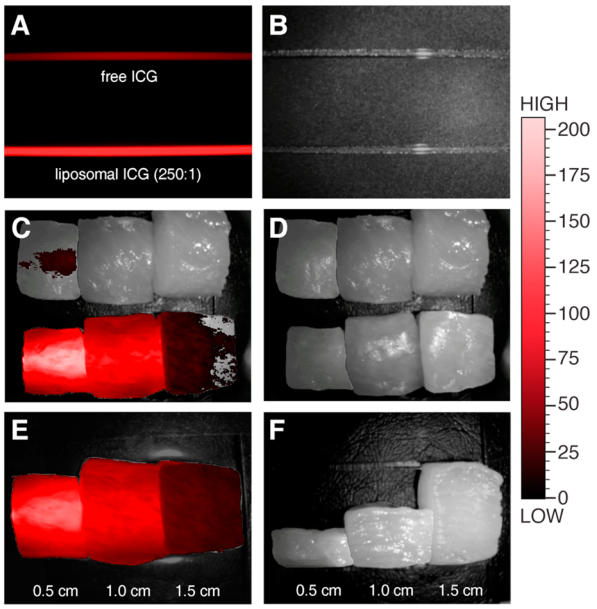

Figure 6. Fluorescence intensity of lipid-bound vs free ICG detected through muscle tissue. (A) NIR fluorescence image intensity of capillary tubes filled with 30 μM free ICG (top) and lipid-bound ICG (bottom). (B) White light image of the two identical capillary tubes filled with different formulations of ICG in panel A. (C) NIR fluorescence image overlaid on a visual light photograph of capillaries filled with free (top) or lipid-bound (bottom) ICG and placed underneath 0.5, 1.0, and 1.5 cm (from left to right, respectively) chicken breast tissue cuboids. (D) Visible light image of chicken breast tissue cuboids in panel C. (E) NIR fluorescence image overlaid on a visual light background of a lipid-bound ICG capillary placed underneath 0.5, 1.0, and 1.5 cm chicken breast tissue cuboids. (F) Side view of tissue cuboid thickness.

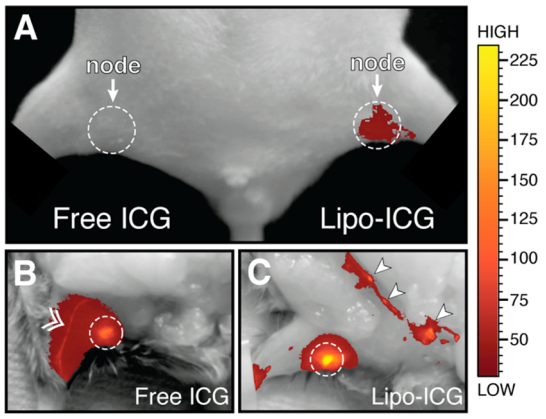

Figure 7. Comparison of lipid-bound ICG and free ICG NIR image behavior in mice after subcutaneous injection. (A) Lipid-bound ICG in liposomes (Lipo-ICG; left foot) or free ICG (right foot) was subcutaneously injected, and the NIR fluorescence image was recorded after 6 min. The fluorescence image is overlaid on a visual light photograph for anatomical representation. The dashed circle indicates the local popliteal node. The mouse is viewed in the supine position. In another set of mice treated with free (B) or lipid-bound (C) ICG for 6 min, the skin was removed and analyzed further. (B) Visible light photograph of the right leg of a mouse treated with free ICG in its right foot. The corresponding fluorescence image is overlaid. The double arrow (≫) denotes the saphenous vein where free ICG appears to diffuse throughout the muscle tissue and the popliteal lymph node (dashed circle). The mouse is viewed in the supine position. (C) Visible light photograph of the right leg of a mouse treated with lipid-bound ICG in its right foot. The corresponding fluorescence image is overlaid. The dashed circle indicates the popliteal lymph node, and bold arrowheads denote ventral pelvic and genital/regional lymph nodes. The mouse is viewed in the supine position.

liposomal form at the same dose. As shown in Figure 7B, 6 min postadministration and after removal of the skin, the animal receiving free ICG showed diffusion of ICG into the blood (saphenous vein). In this case, ICG was clearly detectable in the local popliteal node (Figure 7B). In contrast, in the mouse treated with liposomal ICG, the popliteal lymph node intensity is much higher and a lymphatic track leading to ventral pelvic and genital/regional nodes is readily visible (Figure 7C). The distribution of free ICG to this lymphatic track was not observed.

DISCUSSION

On the basis of the ability of ICG to bind to and insert into a lipid membrane, we have systematically characterized these interactions that confer ICG molecular and fluorescence stability. Our results show that ICG binds to and is incorporated completely and stably into the lipid membrane at lipid:ICG molar ratios as high as a 3:1. At the optimal lipid:ICG ratio of 250:1, we detected a 4.5-fold enhancement of lipid-bound ICG fluorescence intensity versus that of aqueous ICG. At this optimal ratio, liposomal ICG exhibited nearly complete (98%) incorporation efficiency of ICG, and the fluorescence intensity was independent of plasma protein binding. In 4 °C storage away from light, ICG in liposomes was stable [$t_{1/2}$ = 394 days (95% CI, 360−434); $k = 1.76 \times 10^{-3}$ day^{-1} (95% CI, 1.60×10^{-3} to 1.93×10^{-3} day^{-1})] (Figure 5 and Table 1). Liposomal ICG is also stable when exposed to room light for several hours at 25 °C ($t_{1/2}$ = 67.5 ± 11.8 h; k = 0.011 ± 0.002 h^{-1}) (Figure 4). When ICG was administered subcutaneously in mice, preliminary data suggest that lipid-bound ICG exhibited a higher intensity, NIR image resolution, and enhanced lymph node and lymphatic vessel visualization. In contrast, free ICG in mice is readily distributed into the blood with a lower image resolution.

Although ICG in solution can induce liposome aggregation, the exact mechanism is not clear. It is possible that ICG with its high LogP value (6.05 at pH 7.4; low water solubility)[18] may bind to lipid and cause the liposome membrane to become sticky, thus forming liposome aggregations, detected by 90° light scattering and photon correlation spectroscopy as ICG induced an increase in the light scattering and apparent diameter (Figure 1). Others have mixed ICG with preformed liposomes composed of various lipids and observed aggregation[19] or fluorescence enhancement.[14,20] However, these studies did not probe concentration-dependent effects. In our studies, we evaluated and found nonlinear concentration effects and used the information for ICG−liposome admixtures related to ICG−lipid binding and fluorescence enhancement to fine-tune an optimal composition to construct ICG incorporated completely into liposome membranes. We used a well-characterized lipid membrane composed of 90 mol % DSPC and 10 mol % DSPEmPEG$_{2000}$, which is based on a validated and scalable formulation for *in vivo* lymphatic drug delivery.[21] With this lipid composition, we achieved complete incorporation of ICG by mixing ICG and lipids together in the organic phase, producing stable liposomal ICG particles. This is in contrast to other preparations using various lipids where ICG was added in an aqueous solution to encapsulate 50−88.2% of ICG within liposomes.[7−9,22−24] In such situations, some ICG

dx.doi.org/10.1021/bi500021j | *Biochemistry* 2014, 53, 1275−1283

may be trapped within the aqueous compartment while a small fraction may be bound to the lipid membrane.

The observed ICG fluorescence yield enhancement may be related to insertion of ICG within the hydrophobic domains of the lipid bilayer. In hydrophobic organic microenvironments such as methanol, the ICG fluorescence spectrum is reported to have photo- and thermostability.[25] However, the precise ICG−lipid binding configuration that leads to this stabilization is not clear, nor is it known how deep ICG inserts into the lipid membrane. The ICG vertical depth in the lipid membrane could be elucidated by quenching ICG fluorescence with extramembranal iodide ions (KI)[26] or by the parallax method in which quenching of ICG is compared between two strategically placed quenchers at different known carbon positions of the lipid fatty acyl chains.[27] Given the fluorescence enhancement that results from lipid-bound ICG, it is likely ICG inserts at a depth where its interaction with water, which quenches fluorescence and degrades ICG, is minimized. While it is possible that some regions of ICG may be accessible to water and aligned with the phosphate headgroup, it is clear that such interactions did not have a significant impact on the fluorescence yield of ICG. Regardless, ICG embedded in a lipid membrane assumes a conformation that minimizes negative effects on fluorescence properties and the chemical degradation caused by aqueous microenvironments,[6] light, and heat.[25]

While it is clear that insertion into the lipid membrane enhances fluorescence, this enhancement is not unlimited. The nonlinear relationship of fluorescence intensity per ICG versus lipid:ICG molar ratio (Figure 3C) is parabolic with the optimal lipid:ICG molar ratio of 250:1 exhibiting a peak fluorescence yield. The decrease in fluorescence yield to the right side of the vertex correlates with the decreasing ICG density and the amount of ICG available to emit fluorescence. As the density of ICG in the lipid membrane increases, concentration-dependent quenching of ICG may become significant, leading to the observed decline at higher ICG:lipid ratios (or lower lipid:ICG ratios). Because of the significant overlap of the ICG excitation and emission spectra between ∼780 and ∼820 nm (Figure 3A), ICG can undergo self-quenching at high concentrations. However, self-quenching through molecular collision-dependent quenching is unlikely for two reasons. First, ICG is immobilized in a lipid membrane and does not easily collide with other ICG molecules, and second, the experimental concentrations of ICG (40−200 μM ICG in methanol and 0.1−2.0 μM ICG in an aqueous solution) were well below those reported to induce ICG aggregates (dimers). In water, ICG forms dimers at concentrations of ∼5 μM,[3,28−30] and in methanol, ICG forms dimers above 4.2 mM.[29] There may be other molecular interactions that need to be explored further to address the discrepancies. Such studies, however, are beyond the scope of this report.

In addition to optimizing the formulation of liposomal ICG to achieve the maximal fluorescence yield, stability against environmental effects is also necessary. Light causes ICG to produce singlet oxygen that chemically decomposes ICG through a dioxetane reaction (the polymethine chain of ICG cleaves into two carbonyl products, which may be cytotoxic).[25,31] With clinical settings and surgical fields normally well lit, such light decomposition is challenging to avoid. In its currently supplied form, free ICG in aqueous solution decomposes from light in a matter of seconds. Our results show that incorporation of ICG into the lipid membrane shields against light degradation. Liposomal ICG can be exposed to light for several hours at room temperature and retain nearly all of its original fluorescence intensity (Figure 4). To the best of our knowledge, this is the first report of light stability for lipid-bound ICG, and the mechanism for such stability remains to be explored. When stored in the dark at 4 °C in an aqueous suspension, liposomal ICG maintains its fluorescence integrity for at least 8 months (Table 1). This period exceeds those from other reports such as 42 days at room temperature[8] and 70 days at 4 °C.[10] Further stabilization of liposomal ICG could be achieved by lyophilization with a cryoprotectant such as trehalose or sucrose that retains the particle characteristics upon hydration with water. Lipid-bound ICG appeared to be stable in serum as liposomal ICG exposed to 10% heat-inactivated rat serum for 6 h retained 94 ± 0.6% of its initial fluorescence. Taken together, the observed light, storage, and serum stability indicate liposomal ICG has robust stability for clinical use, especially for imaging the lymphatic system where lymph contains a lower serum protein content than blood.

The advantage of NIR fluorescence for biological imaging arises from the minimal autofluorescence of deoxy- and oxyhemoglobin, lipid, and water in the 700−900 nm range. This range is known as the NIR or therapeutic window, and ICG, with its 820 nm emission, is the only FDA- and EMA-approved fluorophore for human use to leverage this property. At present, at least 10 other groups have developed liposomes with ICG incorporated,[10,11,32,33] encapsulated,[8,9,22−24] or adsorbed[20] with lipid membranes of various compositions and physiochemical properties for *in vivo* NIR optical imaging. The polar headgroup of a lipid affects the particle surface charge and degree of hydration, which impacts the level of *in vivo* opsonization and complement binding that induces clearance, and the amount of saturation and chain length of the lipid fatty acyl tails affect the lipid phase transition temperature (T_c) by altering the rigidity, thickness, and uniformity of the lipid bilayer.[12] Therefore, each variable may impact not only the stability and interactions between ICG and lipid but also the *in vivo* behavior of the particles.

In summary, taking advantage of the ability of ICG to incorporate completely and stably into lipid membranes and understanding ICG−lipid interactions, we developed liposomal ICG that maximizes ICG fluorescence intensity and stability. These scalable particles are designed to exhibit physiochemical characteristics suitable for *in vivo* imaging as demonstrated with NIR visualization of lymph nodes. Unlike that of free ICG, because of the physiochemical characteristics of subcutaneously given lipid-bound ICG, liposomal ICG is predominantly localized and distributed within the lymphatics without an initial distribution through the blood. Liposomal ICG could be further developed with surface ligands or antibodies to target diseased cells and tissues in the lymphatic system to visualize these cells, and this liposomal platform may be used to deliver therapeutics. With high storage and light stability, fluorescence intensity, and lymph node imaging resolution compared to those of free ICG, lipid-bound ICG could provide additional medical diagnostic value with NIR optical imaging for early intervention in cases of lymphatic abnormalities.

AUTHOR INFORMATION

Corresponding Author

*Department of Pharmaceutics, University of Washington, Box 357610, Seattle, WA 98195. E-mail: rodneyho@uw.edu. Telephone: (206) 543-3796. Fax: (206) 543-3204.

Funding

Funding provided in part by National Institutes of Health Grants AI77390, RR00166, and RR025014. R.J.Y.H. is also supported by the Milo Gibaldi endowment.

Notes

The authors declare no competing financial interest.

ACKNOWLEDGMENTS

We acknowledge the preliminary work of Jennifer P. Freeling, Cameron Ng, and Danielle Taylor that helped inform the experiments described in this paper. We thank Dr. Satoshi Minoshima for advice on NIR imaging and sharing the CCD NIR imaging device supplied by Hamamatsu.

ABBREVIATIONS

CCD, charge-coupled device; CI, confidence interval; DSPC, 1,2-distearoyl-*sn*-glycero-3-phosphocholine; $DSPEmPEG_{2000}$, 1,2-distearoyl-*sn*-glycero-3-phosphoethanolamine-*N*-methoxy-polyethylene glycol-2000; Egg PC, L-α-phosphatidylcholine; ELS, electrophoretic light scattering; EMA, European Medicines Agency; FDA, Food and Drug Administration; ICG, indocyanine green; NIR, near-infrared; L-ICG, lipid-bound ICG; PCS, photon correlation spectroscopy; SD, standard deviation; SLNs, sentinel lymph nodes.

REFERENCES

(1) Food and Drug Administration (2013) Product Insert: Indocyanine Green (IC-Green™) http://www.accessdata.fda.gov/drugsatfda_docs/label/2006/011525s017lbl.pdf (accessed Jan 6, 2014).

(2) Nguyen, Q. T., and Tsien, R. Y. (2013) Fluorescence-guided surgery with live molecular navigation: A new cutting edge. *Nat. Rev. 13*, 653−662.

(3) Baker, K. J. (1966) Binding of sulfobromophthalein (BSP) sodium and indocyanine green (ICG) by plasma α-1 lipoproteins. *Proc. Soc. Exp. Biol. Med. 122*, 957−963.

(4) Mordon, S., Devoisselle, J. M., Soulie-Begu, S., and Desmettre, T. (1998) Indocyanine green: Physicochemical factors affecting its fluorescence in vivo. *Microvasc. Res. 55*, 146−152.

(5) Zhou, J. F., Chin, M. P., and Schafer, S. A. (1994) Aggregation and degradation of indocyanine green. *SPIE Proceedings. Laser Surgery: Advanced Characterization, Therapeutics, and Systems IV*, 495−505.

(6) Saxena, V., Sadoqi, M., and Shao, J. (2003) Degradation kinetics of indocyanine green in aqueous solution. *J. Pharm. Sci. 92*, 2090−2097.

(7) Proulx, S. T., Luciani, P., Christiansen, A., Karaman, S., Blum, K. S., Rinderknecht, M., Leroux, J. C., and Detmar, M. (2013) Use of a PEG-conjugated bright near-infrared dye for functional imaging of rerouting of tumor lymphatic drainage after sentinel lymph node metastasis. *Biomaterials 34*, 5128−5137.

(8) Proulx, S. T., Luciani, P., Derzsi, S., Rinderknecht, M., Mumprecht, V., Leroux, J. C., and Detmar, M. (2010) Quantitative imaging of lymphatic function with liposomal indocyanine green. *Cancer Res. 70*, 7053−7062.

(9) Jeong, H. S., Lee, C. M., Cheong, S. J., Kim, E. M., Hwang, H., Na, K. S., Lim, S. T., Sohn, M. H., and Jeong, H. J. (2013) The effect of mannosylation of liposome-encapsulated indocyanine green on imaging of sentinel lymph node. *J. Liposome Res. 23*, 291−297.

(10) Sandanaraj, B. S., Gremlich, H. U., Kneuer, R., Dawson, J., and Wacha, S. (2010) Fluorescent nanoprobes as a biomarker for increased vascular permeability: Implications in diagnosis and treatment of cancer and inflammation. *Bioconjugate Chem. 21*, 93−101.

(11) Hua, J., Gross, N., Schulze, B., Michaelis, U., Bohnenkamp, H., Guenzi, E., Hansen, L. L., Martin, G., and Agostini, H. T. (2012) In vivo imaging of choroidal angiogenesis using fluorescence-labeled cationic liposomes. *Mol. Vision 18*, 1045−1054.

(12) Kraft, J. C., Freeling, J. P., Wang, Z., and Ho, R. J. (2014) Emerging research and clinical development trends of liposome and lipid nanoparticle drug delivery systems. *J. Pharm. Sci. 103*, 29−52.

(13) Chang, A. A., Morse, L. S., Handa, J. T., Morales, R. B., Tucker, R., Hjelmeland, L., and Yannuzzi, L. A. (1998) Histologic localization of indocyanine green dye in aging primate and human ocular tissues with clinical angiographic correlation. *Ophthalmology 105*, 1060−1068.

(14) Devoisselle, J. M., Soulie, S., Mordon, S. R., Desmettre, T., and Maillols, H. (1997) Fluorescence properties of indocyanin green. I. In-vitro study with micelles and liposomes. *Proc. SPIE 2980*, 453−460.

(15) Yoneya, S., Saito, T., Komatsu, Y., Koyama, I., Takahashi, K., and Duvoll-Young, J. (1998) Binding properties of indocyanine green in human blood. *Invest. Ophthalmol. Visual Sci. 39*, 1286−1290.

(16) Zheng, X., Xing, D., Zhou, F., Wu, B., and Chen, W. R. (2011) Indocyanine green-containing nanostructure as near infrared dual-functional targeting probes for optical imaging and photothermal therapy. *Mol. Pharmaceutics 8*, 447−456.

(17) MacDonald, R. I. (1990) Characteristics of self-quenching of the fluorescence of lipid-conjugated rhodamine in membranes. *J. Biol. Chem. 265*, 13533−13539.

(18) Chemicalize.org (http://www.chemicalize.org/structure/-!mol=indocyanine+green&source=fp) (accessed January 6, 2014).

(19) Verkade, H. J., de Bruijn, M. A., Brink, M. A., Talsma, H., Vonk, R. J., Kuipers, F., and Groen, A. K. (1996) Interactions between organic anions, micelles and vesicles in model bile systems. *Biochem. J. 320* (Part3), 917−923.

(20) Portnoy, E., Lecht, S., Lazarovici, P., Danino, D., and Magdassi, S. (2011) Cetuximab-labeled liposomes containing near-infrared probe for in vivo imaging. *Nanomedicine 7*, 480−488.

(21) Kinman, L., Brodie, S. J., Tsai, C. C., Bui, T., Larsen, K., Schmidt, A., Anderson, D., Morton, W. R., Hu, S. L., and Ho, R. J. (2003) Lipid-drug association enhanced HIV-1 protease inhibitor indinavir localization in lymphoid tissues and viral load reduction: A proof of concept study in HIV-2287-infected macaques. *J. Acquired Immune Defic. Syndr. 34*, 387−397.

(22) Turner, D. C., Moshkelani, D., Shemesh, C. S., Luc, D., and Zhang, H. (2012) Near-infrared image-guided delivery and controlled release using optimized thermosensitive liposomes. *Pharm. Res. 29*, 2092−2103.

(23) Zhuang, Y., Ma, Y., Wang, C., Hai, L., Yan, C., Zhang, Y., Liu, F., and Cai, L. (2012) PEGylated cationic liposomes robustly augment vaccine-induced immune responses: Role of lymphatic trafficking and biodistribution. *J. Controlled Release 159*, 135−142.

(24) Suganami, A., Toyota, T., Okazaki, S., Saito, K., Miyamoto, K., Akutsu, Y., Kawahira, H., Aoki, A., Muraki, Y., Madono, T., Hayashi, H., Matsubara, H., Omatsu, T., Shirasawa, H., and Tamura, Y. (2012) Preparation and characterization of phospholipid-conjugated indocyanine green as a near-infrared probe. *Bioorg. Med. Chem. Lett. 22*, 7481−7485.

(25) Holzer, W., Mauerer, M., Penzkofer, A., Szeimies, R. M., Abels, C., Landthaler, M., and Baumler, W. (1998) Photostability and thermal stability of indocyanine green. *J. Photochem. Photobiol. 47*, 155−164.

(26) Bronshtein, I., Afri, M., Weitman, H., Frimer, A. A., Smith, K. M., and Ehrenberg, B. (2004) Porphyrin depth in lipid bilayers as determined by iodide and parallax fluorescence quenching methods and its effect on photosensitizing efficiency. *Biophys. J. 87*, 1155−1164.

(27) Chattopadhyay, A., and London, E. (1987) Parallax method for direct measurement of membrane penetration depth utilizing fluorescence quenching by spin-labeled phospholipids. *Biochemistry 26*, 39−45.

(28) Li, X., Beauvoit, B., White, R., Nioka, S., Chance, B., and Yodh, A. (1995) Tumor localization using fluorescence of indocyanine green (ICG) in a rat model. *Proc. SPIE 2389*, 789−797.

(29) Philip, R., Penzkofer, A., Baumler, W., Szeimies, R. M., and Abels, C. (1996) Absorption and fluorescence spectroscopic investigation of indocyanine green. *J. Photochem. Photobiol., A 96*, 137−148.
(30) Rajagopalan, R., Uetrecht, P., Bugaj, J. E., Achilefu, S. A., and Dorshow, R. B. (2000) Stabilization of the optical tracer agent indocyanine green using noncovalent interactions. *Photochem. Photobiol. 71*, 347−350.
(31) Engel, E., Schraml, R., Maisch, T., Kobuch, K., Konig, B., Szeimies, R. M., Hillenkamp, J., Baumler, W., and Vasold, R. (2008) Light-induced decomposition of indocyanine green. *Invest. Ophthalmol. Visual Sci. 49*, 1777−1783.
(32) Murata, M., Tahara, K., and Takeuchi, H. (2013) Real-time in vivo imaging of surface-modified liposomes to evaluate their behavior after pulmonary administration. *Eur. J. Pharm. Biopharm.*, DOI 10.1016/j.ejpb.2013.09.006.
(33) Zanganeh, S., Xu, Y., Hamby, C. V., Backer, M. V., Backer, J. M., and Zhu, Q. (2013) Enhanced fluorescence diffuse optical tomography with indocyanine green-encapsulating liposomes targeted to receptors for vascular endothelial growth factor in tumor vasculature. *J. Biomed. Opt. 18*, 126014.